

Gradient Pattern Analysis of Asymmetric Fluctuations: Applications for Short Time Series and Disordered Spatial Structures

Rosa, Reinaldo R.

National Institute for Space Res. –INPE, Lab for Computing and Applied Mathematics-LAC
Av. dos Astronautas, 1758, São José dos Campos, SP, CEP 12227-970, Brazil
reinaldo@lac.inpe.br

Introduction

The Gradient Pattern Analysis (GPA) is an innovative technique, which characterizes variability patterns, in time and space, based on large and small amplitude fluctuations of the spatial, temporal, and spatio-temporal structures represented as a static or dynamical gradient lattice (Rosa et al, 1999; Rosa et al. 2003). In this approach, a given scalar field of fluctuations can be represented as a composition of four gradient moments, as given by Rosa et al. (2003). According to the GPA methodology, the first gradient moment g_1 (here we call it G), a measurement of asymmetric fluctuation called here *asymmetry coefficient* G , is given by: $G = |\varepsilon - f| / f$, with $\varepsilon \geq f > 0$, where f is the number of asymmetric fluctuations and ε is the geometric energy correlation given by the number of connections among all fluctuations. The geometric connection among the fluctuations is generated by a Delaunay triangulation taking the middle points of the asymmetric vectors as vertices. Due to the possible changes in the phases of each fluctuation (a vector in the gradient lattice) the parameter ε is very sensitive in detecting local asymmetric fluctuations on the gradient lattice. Two remarkable applications of GPA's first gradient moment, G , are organized in this work as follows: (i) By analyzing canonical temporal variability patterns we show that the new method can reliably characterize the phenomenological dynamical process of short time series ($N \leq 10^3$ measurements). Based on the combination of GPA and wavelet decomposition (Percival and Walden, 2000) we introduce the concept of *gradient spectra* from where it is possible to estimate the mutual information distance. As an example of application in space science data analysis, we show that the fluctuation pattern of the short and weak impulsive solar burst, with low energetic amplitudes, is closer to the colored noise variability pattern with power spectrum $P(k) \sim k^{-5/3}$. (ii) Also based on the combination of GPA and wavelets, we have introduced a new measurement that allow us to characterize disordered patterns in 2d space for that it is know a reference ordered pattern. Numerical solutions of KPZ stochastic equation and Scanning Force Microscopy (SFM) patterns of porous silicon samples are analyzed using this methodology.

Time Series

Fig. 1 shows the normalized selected 3GHz short solar burst pattern (SBP), composed by 512 measurements, that has been analyzed in this paper. Due to its short composition it is impossible to characterize the robustness of its turbulent power-law.

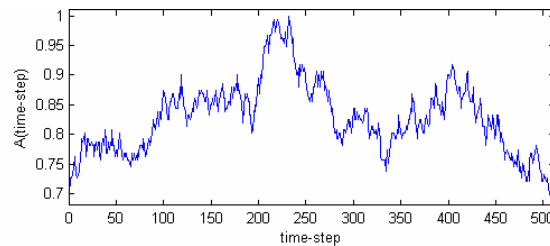


Figure 1: The short 3GHz impulsive radio burst event with normalized amplitude.

In order to characterize the fluctuation pattern of the SBP time series, showed in Fig. 1, we selected two turbulent-like variability patterns generated from the stochastic systems as given by Osborne and Provenzale (1989). In numerical theory of $1/\omega$ noise the spectrum of the stochastic process is sampled into a discrete series of frequencies and the random function is then computed as a discrete series at times $t_i = i \Delta t$, $i = 1, \dots, M$. Thus, given a power spectrum of a random function ω_k , $P(\omega_k) \sim \omega_k^{-\alpha}$, characterized by the spectral index α , they define the correspondent real random time series by simple superposition of harmonic oscillations (they represent a class of *fractional Brownian fluctuation of index α* with turbulent-like

variability patterns). Two examples were normalized, one for $\alpha = 2$ and the other for $\alpha = 5/3$, and they are shown in Figures 2a and 2b, respectively.

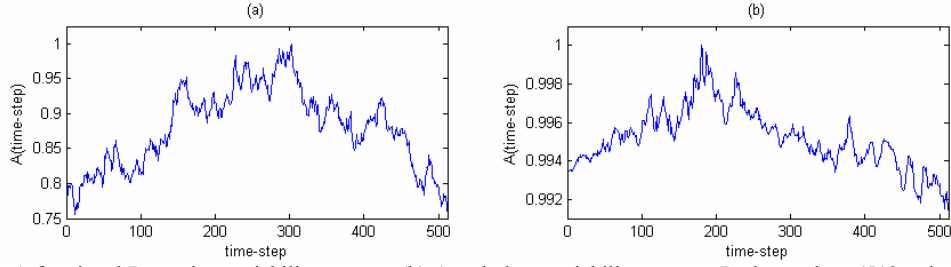


Figure 2: (a) A fractional Brownian variability pattern; (b) A turbulent variability pattern. Both are short (512 points) and have an equivalent clustered impulsive profile pattern as the solar radio burst showed in Figure 1 b.

Usually the characterization of irregular fluctuations from time series, as given by turbulent-like profiles, is performed specifically on the kurtosis measures from the respective PDF. For that, it is necessary to have time series composed of $\sim 10^4$ points. For time series the GPA operation is straightforward and brings some advantages on the traditional methodologies. The asymmetry coefficient G is intrinsically calculated on the amplitude differences (fluctuations) given by the gradient pattern. As the first gradient moment is very sensitive to small changes in the phase and modulus of each fluctuation vector, it can distinguish complex variability patterns even when they are very similar and consist of a low amount of vectors (Assireu et al., 2002). As the SBP profile under investigation in this paper is composed of only 512 measurements its respective matrix of fluctuations, in order to get the square correspondent minimum gradient lattice (22×22), must be constructed by taking 484 points. Note that 512 are not reducible to a square gradient lattice $L \times L$. This procedure can be conducted by taking the points from left to right or vice-versa, without loss of significant information. Thus, from each 484 measurements a value for G parameter is calculated from the operation on the respective square gradient lattice 22×22 . All the signals considered in this analysis are rich in scales where the information about higher-order joint probability densities and self-affine dimensions are hidden. Our second-step consists in obtaining the values of asymmetric coefficient for each inherent frequency of the signal. Thus, in such cases we can have the asymmetry coefficient as a function of frequency $G(\omega)$. Thus, using a DB8 decomposition (Daubechies, 1990) the components of our time series were obtained following a dyadic scale giving nine decompositions ($2^9=512$) where the frequencies are $1/2, 1/4, 1/8, 1/16, \dots, 1/512$. Once we have defined how to decompose each original time series in a set of nine scaling characteristic time series, the next step in our operation is to obtain the respective gradient spectra by computing the respective asymmetry coefficients. Thus, for each set of decomposition it is possible to calculate the respective asymmetry coefficient G , so that for each signal it is possible to have the asymmetry coefficient as a function of the characteristic frequencies ω , $G(\omega)$. Thus, the gradient spectrum, obtained from a N -measurements time series, consists of ℓ values of $G: \{G(\omega_1), \dots, G(\omega_\ell)\}$ where ℓ is the amount of discrete decomposed time series from the original signal, having $2^\ell=N$. In our case we have $\ell=9$ and then the respective gradient spectrum $\{G(\omega_1), \dots, G(\omega_9)\}$ can be plotted in the $G \times \log_{10}(\omega)$ space. For a given decomposed signal, the search for its best gradient spectrum is well performed by interpolating the ℓ points using a cubic spline fitting and then we can resample the original ℓ -points gradient spectrum by a denser set of points. This, of course, costs much less computationally than using a continuous wavelet transform to obtain the gradient spectrum and, for our analysis, the denser resample procedure is necessary to estimate, with high precision, the normalized mutual information distance between a pair of gradient spectra. Thus, based on the concept of relative information (Kullback and Leibler, 1951), the normalized mutual information distance is defined here as $\delta_N = (1/N) \sum \chi_n \ln(\chi_n / \rho_n)$, where ρ_n is the reference discrete gradient spectrum (in this paper, it is alternatively the gradient spectra for one of the canonical time series) and χ_n is the discrete gradient spectrum to be characterized (in this paper, it is the gradient spectrum for the SBP time series). In Fig. 3 we can appreciate each characteristic gradient spectrum: weak turbulence (Δ), strong turbulence (\times) and SBP (\circ).

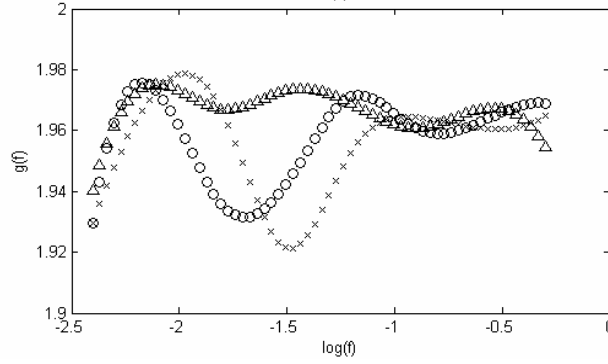


Figure 3: The mutual gradient spectra obtained from the decomposition of each time series: solar burst (circle), turbulent (cross) and Brownian (triangle).

The values of δ_N obtained having χ_n as the SBP are $\delta_N(\chi|\rho_{\alpha=2})=0.061\pm0.002$ and $\delta_N(\chi|\rho_{\alpha=5/3})=0.016\pm0.002$. Thus, comparing these values for δ_N we found the SBP closer to the strong MHD turbulent-like pattern variability (Galtier et al., 2002). Performing calculations for distinct groups of short stochastic *fluctuations*, we obtained a average mutual information distance of 0.08 ± 0.01 between their respective gradient spectra.

Gradient Pattern Analysis of Spatial Structures

Formation of surfaces is influenced by a large number of factors, where randomness plays an essential role in shaping the final morphology of a given surface or interface. Recently, the so-called KPZ equation has been used to model the surface of porous silicon (Baroni et al, 2006). The GPA of the modeled surfaces showed that it is possible to reproduce, with good approximation, the disordered character of the porous surfaces by means of the numerical solution of KPZ equation (Kardar, Parisi and Zhang, 1986). Thus, based on conventional scaling analysis for porous surfaces, here we introduce a complementary methodology to improve this characterization. The data to test our methodology are porous silicon samples, SP83 and SP101 (see Fig. 4a and 4b) produced by anodic etching of crystalline silicon wafers in hydrofluoric (HF) acid solution. These samples were analyzed by Scanning Force Microscopy (SFM) to obtain the morphology of the porosity. An equivalent KPZ solution is shown in Fig. 4c. The emphasis here is on the characterization of a relative structural complexity of porous silicon samples and possible correspondent generic models. For this purpose was considered, for comparison criteria in nanoscales, a reference sample of Au film deposited under ultra-high vacuum conditions on air-cleaved mica substrate (Fig. 4d).

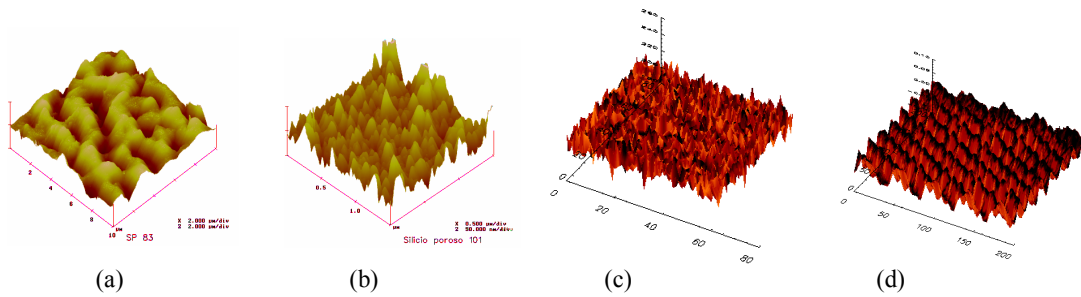


Figure 4 – (a) Psi SFM surface from sample 83 (low roughness); (b) Psi SFM surface from sample 101 (high roughness); (c) a typical nano-KPZ surface; (d) a regular gold on mica deposition surface showing low structural complexity – Au_Mica;

In the context of spatial data, the local fluctuation, between each pair of amplitudes of the global pattern is characterized by its gradient vector at corresponding mesh-points in the two-dimensional space. In this representation, the relative values between adjacent amplitudes (“local fluctuations”) are relevant, rather than the respective absolute values. Thus, the measurement of asymmetric fluctuation by means of the *asymmetry coefficient G*, is considered. In this approach each local fluctuation is represented by a vector in a 2d-space. The asymmetry coefficient *G* is intrinsically calculated on the amplitude differences (fluctuations) given by the gradient pattern of the spatial structure. As the asymmetry coefficient is very sensitive to small changes in the phase and modulus of each fluctuation vector, it can distinguish complex

variability patterns even when they are very similar and consist of a low amount of vectors. Once the 2D spatial patterns can be decomposed into different frequency sub-bands, it may be interesting to characterize a gradient spectrum by calculating the asymmetry coefficient for the sub-matrices that can be obtained from such scaling decomposition. Here, we use the wavelet multiresolution analysis (WMA) in 2D space with a decomposition methodology introduced by Guan et al (2002). Each original pattern can be described by a scalar field from where 2D subspaces can be divided into LL, LH and HL and HH components (H for *high-pass* and L for *low-pass*), thus an image is a square integrable function that can be decomposed into appropriate subspace components characterized by the frequencies f_{\max} , $f_{\max}/2$ (HH₃), $f_{\max}/4$ (HH₂), and $f_{\max}/8$ (HH₁). In our notation, considering $f_{\max} = 1$, we use the reference values of 1, 0.5, 0.25 and 0.125. As we have a sub-matrix for each one of the frequencies, we can calculate the asymmetry coefficient as a function of f , generating the following spectra: $G: \{G(1), G(0.5), G(0.25), G(0.125)\}$ that we call *gradient spectrum*. The calculated gradient spectra for the samples (SP83, SP101, KPZ and Au_MICA) are shown in Figure 5. In that sense our results work as a validation criterion for modeling.

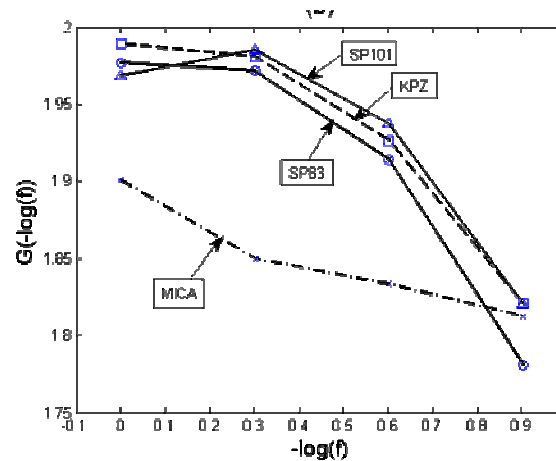


Figure 5 –The Asymmetry spectra of the samples which are shown in Fig. 4.

Concluding Remarks

Our analysis, based on an innovative methodology called *gradient spectral analysis*, has been applied in classifying the time variability profile of short time series (here, a solar radio burst variability interpreted as a result of strong MHD turbulent-like pattern, a process with spectral index $\alpha=5/3$). It is hoped that the analysis presented here will prove useful in investigations of short complex time series and the addition of statistical significance tests will improve both quantitative and qualitative phenomenology of gradient spectral analysis. Further improvement of this methodology, for 1D and 2D, which could lead more precise relative structural complexity characterization, might involve other reference patterns as random (Gaussian and non-Gaussian fluctuations), chaotic dynamics, ballistic deposition, sine combination surfaces, among others.

Acknowledgments: The work was financially supported by INPE-MCT and CNPq. The author acknowledges the data from EMBRAPA, UFBA and Ondrejov Observatory, and the discussion and computational work from NUSASC-LAC team.

References

- Assireu, A.T., et al. *Physica D* 168(1):397-403, 2002.
- Baroni, M.P.M.A. et al. *Microelectronics Journal* 37:290-294, 2006a.
- Daubechies, I., *IEEE Trans. Inform. Theory* 36:961-1004, 1990.
- Galtier, S.; Nazareno, S.V.; Newell, A.C.; Pouquet, A., *Astroph. Journal* 564 :L49-L52, 2002.
- Guan, S.; Lai, C.-H.; Wei, G. W. *Physica D*, v. 163, p. 49-79, 2002.
- Kardar, M.; Parisi, G.; Zhang, Y.-C., *Phys. Rev. Lett.* 56:889-892, 1986.
- Kullback, S., Leibler, R.A., *Annals of Mathematical Statistics* 22(1):79-86, 1951.
- Osborne, A.R., Provenzale, A., *Physica D* 35:357-381, 1989.
- Panchev, S., *Random Functions and Turbulence*, Pergamon, Oxford, 1971.
- Percival, D., Walden, A., *Wavelets Methods for Time Series Analysis*, Cambridge, 2000.
- Rosa, R.R., Sharma, A.S., Valdivia, J.A., *Int. J. Mod. Phys. C* 10: 147-163, 1999.
- Rosa, M.R. Campos, F.M. Ramos, S. Fujiwara, T. Sato, *Braz. J. Phys.* 33:605-609, 2003.